Innovative Infrastructure Solutions (2024) 9:63
https://doi.org/10.1007/s41062-024-01369-w

TECHNICAL PAPER

Exploring the impact of nano-limestone cementitious material on mechanical, infiltration, and microstructure properties of pervious concrete

Gowhar Afzal[1] · **Tanveer Rasool**[1]

Received: 2 September 2023 / Accepted: 9 January 2024 / Published online: 10 February 2024

Abstract
The impact of nano-limestone (NL) on the properties of pervious concrete (PC) is the focus of this study. The work explores workability, paste drain down, porosity via CT scanning, hardened density, mechanical strength, infiltration, and microstructural properties of PC. Field emission scanning electron microscopy, X-ray diffraction, and Fourier transform infrared spectroscopy facilitated the microstructural analysis. The findings verified that NL served as an inert substance that enhanced the density of the microstructure in PC. Moreover, it expedites cement hydration process by promoting the generation of nuclei at the boundaries. Different replacement rates of NL (1%, 2%, 3%, and 4%) were examined concerning cement. At a 2% NL replacement, the measured compressive strength of PC was 12.12 MPa and 24.29 MPa after 3 and 28 days, respectively. Splitting tensile strength recorded values of 1.62 MPa and 3.12 MPa, while shear strength measured 1.92 MPa and 3.75 MPa for the same periods. Significant enhancements were observed with compressive strength increasing notably by 48.2% after 3 days and 19.2% after 28 days. Similarly, the splitting tensile and shear strengths displayed remarkable increments of 48.6% and 16.4% after 3 days and 58.6% and 26.4% after 28 days, respectively. However, an increased NL percentage resulted in reduced permeability, rendering PC nearly impermeable at 4% replacement. The optimal NL percentage to maintain PC permeability was $\leq 2\%$, preserving an infiltration rate of 2.43 mm s^{-1}.

Keyword Infiltration rate · Mechanical properties · Microstructure · Nano-limestone · Pervious concrete

Introduction

Cement production is likely to increase in future, releasing CO_2 into the atmosphere. Hence, a proper and sustainable practice is necessary to control the excess production of cement and its impact on the environment [1, 2]. The use of nano-materials in normal and pervious concrete as the replacement of basic ingredients like cement or as a blend has shown potential for improvement in both mechanical and durability properties of concrete, thereby helping to decrease cement usage that can indirectly lead to a reduction in cement production [2]. The same is credited to the very high surface area of nano-materials than the macro materials. The nano-materials are reported as highly reactive and thus quickly enhance the mechanical properties of the blends. The basic mechanism for improving properties is based on the nucleation sites for forming nano-calcium silicate hydrate (CSH) gel. CSH gel acts as a nano-material in the concrete by filling nano-pores, thereby acting as nano-reinforcement, enhancing the hydration process and durability [3]. Nanotechnology thus provides wide scope for improvement in the properties of traditional and specially designed porous concrete. Porous concrete, commonly known as pervious concrete, contains cement, coarse aggregates, water, and very little or no fine aggregates. However, unlike normal concrete, it is a composite with a void ratio of 15–25% [4, 5]. The primary goal of pervious concrete (PC) is to create a system of continuous interconnected pore structure, typically accomplished by reducing or fully eliminating the amount of fine aggregates and only cement, coarse aggregates, and water are used. To achieve bonding between adjacent particles, the coarse aggregates must be coated with an optimal

✉ Tanveer Rasool
tanveer@nitsri.ac.in

Gowhar Afzal
gowhar_11phd19@nitsri.ac.in

[1] Department of Chemical Engineering, National Institute of Technology, Srinagar 190006, India

amount of cement paste [6–9]. Some advantages of pervious concrete include the reduction of stormwater runoff through infiltration recharging of the groundwater, reducing the need for uneven drainage system, helping in water filtration and reducing water pollution caused by runoff [10]. Pervious concrete (PC) has been regarded as one of the best management practices (BMPs) to take hold of stormwater runoff due to its high permeability, which aids in reducing stormwater runoff and helps recharge groundwater [11–13]. Although pervious concrete (PC) is an alternative to overcome the above-listed problems, the lesser compressive strength along with the clogging of the pervious concrete (PC) is the challenging factor which needs to be addressed [14]. As per ACI Chapter-1, the compressive strength of pervious concrete lies between 2.8 and 28 MPa, which is very less when compared to normal concrete, 17 to 40 MPa [15]. Improvement of mechanical and permeable properties using fibre with different compaction techniques and short-duration vibration techniques have shown improved mechanical properties because of the formation of viscous layers between cement matrix and aggregate grains [16]. Similarly, to improve the performance of pervious concrete (PC), several materials like blast furnace slag (BFS), flue gas desulfurisation gypsum (FGDG), and fly ash (FA) have been studied by researchers as binders in pervious concrete (PC) and the various properties, which include microstructure, mechanical, and durability properties have been investigated using X-ray diffractometer (XRD), scanning electron microscope (SEM), and other standard methods [17].

The addition of nano-materials like nano TiO_2 in concrete has revealed the self-cleaning property of the pervious concrete (PC), thus lowering the clogging of the pervious concrete (PC) to some extent [18]. Using nano-silica has shown good performance, enhancing porous concrete pavement's strength, clogging, and durability through pore-filling and pozzolanic properties [19, 20]. Using carbon nanotubes (CNTs) in porous concrete pavements has enhanced pervious concrete (PC) thermal conductivity and mechanical properties [18]. Nanotubes, carbon nano-fibers, nano ZrO_2, nano TiO_2, nano SiO_2, and nano Al_2O_3 are a few key nano-materials, more precisely reported as replacements of cement in aggregates [21]. The utilisation of nano-materials in normal and pervious concrete has garnered significant attention due to their potential for enhancing the properties of this essential construction material. However, one of the main challenges hindering their widespread adoption is the high cost associated with certain nano-materials used in concrete [22]. Materials such as carbon nano-tubes (CNTs), graphene, and nano-silica are considered at the forefront of innovation in this field but are also known for their high production costs. For instance, synthesising CNTs and graphene requires specialised techniques and equipment, increasing manufacturing expenses. Similarly, nano-silica production involves sophisticated processes, contributing to its elevated cost. These high costs associated with nano-materials pose a significant barrier to their practical implementation in the construction industry, limiting their availability and impeding their potential impact on improving pervious concrete properties [23]. Previous research primarily focused on utilising micro calcite, the purest and most stable calcium carbonate ($CaCO_3$) state. This compound has been recognised for its chemical reactivity, accelerating the hydration process and enhancing traditional cement-based substance's fresh/early-age strength [24]. In ultrahigh performance concrete (UHPC), nano-silica (NS) and nano-limestone (NL) as cement substitutes displayed distinct roles. Nano-silica (NS) acted as a potent filler, reducing porosity and accelerating cement hydration, while nano-limestone (NL) enhanced microstructure density. Optimal nano-silica (NS) and nano-limestone (NL) contents around 1.0% and 3.0%, respectively, yielded maximum UHPC mechanical strengths, emphasising their critical influence on UHPC matrix performance [25]. Similarly, it has also been studied that nano-limestone (NL) substantially speeds up early cement hydration, with a direct correlation between the quantity of nano-limestone (NL) and the extent of acceleration [26]. It has been proposed that limestone, which consists predominantly of $CaCO_3$, could be used as a partial replacement for cement without significantly impacting the hydration process (which involves the chemical reaction between cement and water). However, it helps it to speed up at an early stage and compressive strength. In European cement production, limestone is commonly used due to its availability and beneficial properties. However, in North America, its use is restricted by cement standards, such as those set by ASTM [27]. The Canadian Standards Association has been discussing protocols for incorporating limestone additives in cement-based materials, including permissible limits for various applications and environments [28]. Conversely, ever since the advent of various nano-materials, the concrete sector has invested significantly in exploring the effects and potential applications of nano-materials in concrete [18]. One advantage of nano-calcium carbonate over other nano-materials is its comparatively reasonable cost [22]. However, limited studies have investigated the impact, benefits, and potential applications of incorporating nano-calcium carbonate in pervious concrete.

Research significance

A brief examination of the literature, as offered in the preceding section, reveals that many studies have already been carried out to augment the mechanical properties of pervious concrete (PC) made with various nano-materials. However, the limited availability of literature on usage of nano-limestone

(NL) as a filler and cement replacer in pervious concrete (PC), exclusively on its mechanical, infiltration, and microstructural properties, has been a motivating factor of the present study. The study will also be helpful to overcome the limitations associated with other nano-materials, their high cost, and less availability. Hence, the present study's main objectives were to pulverise the locally available limestone rock into nano limestone powder using a specially designed ball mill and develop a pervious concrete mix with optimum mechanical, infiltration, and microstructural properties. The mechanical strength evaluations, including tests for compressive, tensile, and shear strength, were carried out on both pervious concrete (PC) and modified pervious concrete (PC) mixes at different time intervals during the curing process: 3, 7, 14, and 28 days. However, tests for infiltration rate, hardened density, and porosity were conducted specifically after 28 days of curing. The microstructure analysis was performed using a field emission scanning electron microscope (FE-SEM), X-ray diffraction (XRD), and Fourier transform infrared spectroscopy (FT-IR) on 28 days cured samples. Moreover, a novel technology using CT scanning of the hardened pervious concrete (PC) was carried out to check its porosity. The immediate testing after mixing involved evaluating fresh properties such as workability and paste drain down test. The economic feasibility of the designed mixes was also checked through cost analysis by finding the economic index (EI). The findings suggest that the nano-limestone (NL) modified pervious concrete developed in this study could provide remuneration to various stakeholders in the construction industry.

Materials and test methods

Materials

This study used the basic components of the concrete, like OPC grade 53, coarse and fine aggregate, water and the replacement material as nano-limestone. The nano-limestone was used as a substitute for cement partially. The nano-limestone (NL) was prepared through pulverisation and then characterised; the material's description is below.

A well-ground OPC of 53 grade was chosen for its better strength, conforming to IS 12269-(1987) [29]. The 53 grade OPC also possessed lower %age of sulphates and chlorides; for obtaining the chemical composition of OPC grade 53, X-ray fluorescence spectrometer was used. The results are summed in Table 1, and the physical properties are presented in Table 2. The role of fine aggregates is as a workability agent while filling the voids of coarse aggregates. The fine aggregate used in the present study was river sand, falling in the range of 90 micron-2.36 mm, 90-micron retaining and 2.36 passing with a fineness modulus of 2.38 conforming to zone II. The coarse aggregates used were in size range of 4.75–15 mm, free from dust and other undesired materials, conforming to IS 383-(2016) [30]. The physical properties of aggregates are summed in Table 3, and the gradation curve of coarse aggregates is presented in Fig. 1. The portable water confirming the IS: 456-2000 [31] was utilised in the experiments. The tools do on the samples ensured that the water was free from oils, acids, salts and alkalis, which may affect the pervious concrete (PC) properties.

Preparation of nano-limestone (NL)

Limestone (LS) is a naturally occurring calcium sedimentary stone with a higher percentage of minerals such as calcite and aragonite. The percentage of calcite is between 80 and 90% for most limestone rocks. The state of J&K India has many unexplored limestone reservoirs. The locally available LS from one of the reservoirs south to the city of Srinagar, Lower Munda Qazigund, was collected and prepared to be used as a partial replacement of cement in pervious concrete (PC).

The limestone was initially cleaned using acetone and distilled water and then oven dried for 3 h at 60 °C to remove the surface moisture from the limestone, then the adequate amount (17.063 g) of limestone sample was taken for pulverisation using a specially designed ball mill (Planetary 5, FRITSCH) to obtain nano-sized limestone, two silicon nitride jars were used having a volume of 500 ml, each jar contains (8.533 g) of the sample with 44 number of balls. A total of eighty-eight silicon nitride balls were utilised for the effective crushing and grinding of limestone samples. Different-sized balls were used with an average weight of 1.939 g. The ball and sample ratio were taken as 10:1, and

Table 2 Physical properties of OPC 53

Properties	Cement	Testing standards	Code
Setting time			
i. Initial (min)	49	IS: 12269-(1987)	[29]
ii. Final (min)	284		
Specific gravity	3.15	IS: 12269-(1987)	–
Normal consistency (%)	27.7	IS: 12269-(1987)	–
Soundness (mm)	2	IS: 12269-(1987)	–
Specific surface area (cm^2/g)	3371	IS: 12269-(1987)	–

Table 1 X-ray fluorescence analysis of OPC grade 53

Constituents	CaO	SiO_2	Al_2O_3	Fe_2O_3	SO_3	MgO	K_2O	Na_2O	TiO_2	Other oxides
Percentage	65.62	19.50	4.88	3.86	2.47	1.83	0.88	0.24	0.33	0.39

Table 3 Physical properties of the aggregates

Properties	Coarse aggregates	Fine aggregates	Testing standards	Standards
Soundness (%)	5.4	–	BIS (2002)	[32]
Crushing value (%)	16.6	–	IS: 2386 (Part IV) (2016)	[33]
Abrasion value (%)	15.0	–	ASTM C131M-20 (2014)	[34]
Impact value (%)	13.2	–	IS: 2386 (Part IV) (2016)	[33]
Water absorption (%)	1.5	2.5	ASTM C 128-01 (2001)	[35]
Fineness modules	7.22	2.38	IS: 2386 (Part IV) (2016)	[33]
Specific gravity (SG)	2.78	2.67	IS: 2386 (Part IV) (2016)	[33]
Zone	–	II	IS: 383 (2016)	[30]
Colour	Grey	–	IS: 2386 (Part IV) (2016)	[33]

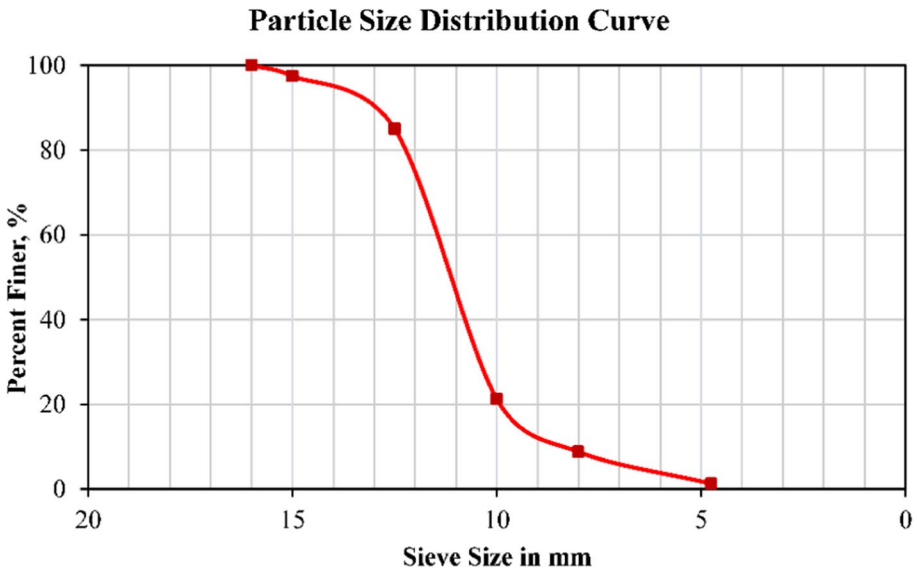

Fig. 1 Gradation curve of coarse aggregates

the pulverisation was carried out for 4 h, at an rpm of 350, with a pause of 15 min after every hour of operation. Figure 2a represents the physical change in limestone. After desired pulverisation, the sample was stored in air-tight containers for further usage.

Nano-limestone (NL) was characterised using various techniques, including field emission scanning electron microscopy (FE-SEM), particle size analyser, X-ray diffraction (XRD), and Fourier transform infrared spectroscopy (FT-IR), and the results are presented in Fig. 2a–e.

SEM analysis revealed that the nano-limestone (NL) particles exhibited a uniform size distribution with an average diameter of approximately 60 nm, evident from particle size analysis. The SEM images also showcased a spherical morphology with a smooth surface, indicating well-dispersed nano-particles. XRD analysis confirmed the presence of pure calcium carbonate in the nano form, as evidenced by the characteristic diffraction peaks at 2θ values of 29.4°, 36.3°, and 47.8°, corresponding to the crystallographic planes (103), (111), and (112) of calcite, respectively, indicated the successful preparation of nano-limestone (NL) with a highly crystalline structure. FT-IR spectra exhibited prominent absorption bands at around 712 cm^{-1} and 875 cm^{-1}, corresponding to the stretching vibrations of the carbonate (CO_3^{2-}) groups, further confirming the presence of calcium carbonate. Additionally, the FT-IR analysis revealed additional peaks at 1400–1500 cm^{-1}, indicating the presence of adsorbed water molecules on the surface of nano-limestone (NL). Overall, the combination of FE-SEM, particle size analyser XRD, and FT-IR characterisation techniques provided comprehensive information about the size, morphology, crystallinity, and chemical composition of the nano-limestone (NL), facilitating its precise evaluation.

Mix design

The design mix was prepared using the weight approach method. The locally available limestone ground to nano level was used as a replacement material for cement to certain proportions in the mix designs. Five mixes were

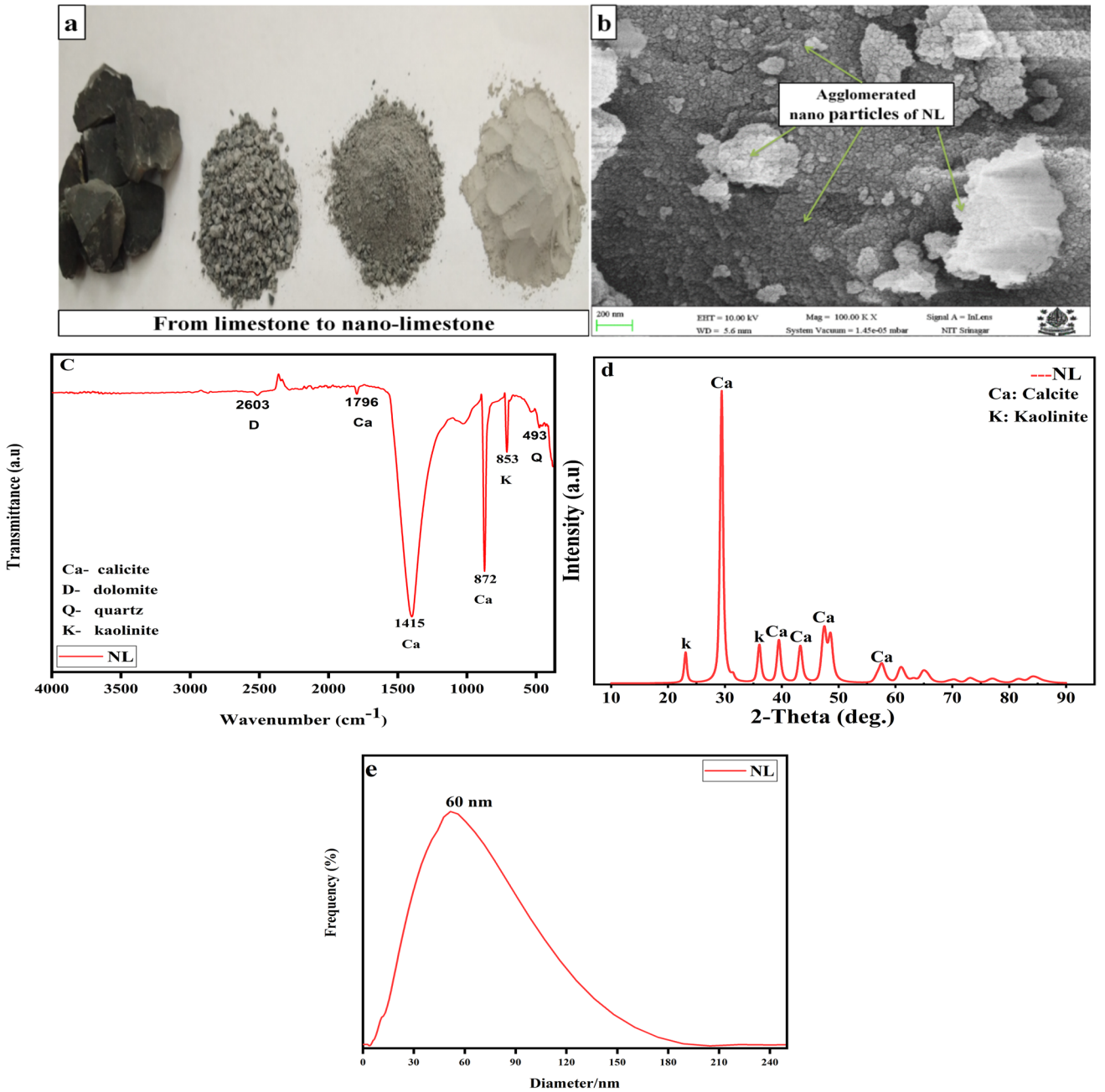

Fig. 2 **a** Physical changes in LS, **b** FE-SEM micrograph of NL, **c** FT-IR spectrum of NL, **d** XRD pattern of NL, and **e** particle size analysis of NL

used, including normal mix PC0NL (pervious concrete with 0% nano-limestone (NL)), followed by four other mixes PC1NL (pervious concrete with 1% nano-limestone (NL)), PC2NL (pervious concrete with 2% nano-limestone (NL)), PC3NL (pervious concrete with 3% nano-limestone (NL)), and PC4NL (pervious concrete with 4% nano-limestone (NL)) by weight of cement as per the specifications laid down in ACI 522R-10 [15]. The description of all the mixes is presented in Table 4. The minimum and maximum range of the aggregates was fixed between 4.75 to 15 mm, respectively, whereas the W/C ratio was fixed at 0.35.

Table 4 Mix design for kg/m^3 of PC and modified PC mixes

Mix description	C/CA	OPC (C)	Coarse aggregate (CA)	NL	W/C ratio	Water	Fine aggregates (FA)
PC0NL	1:4	404.6	1456.8	0.0	0.35	141.6	161.8
PC1NL	1:4	400.5	1456.8	4.04	0.35	141.6	161.8
PC2NL	1:4	396.5	1456.8	8.09	0.35	141.6	161.8
PC3NL	1:4	392.4	1456.8	12.13	0.35	141.6	161.8
PC4NL	1:4	388.42	1456.8	16.18	0.35	141.6	161.8

Test methods

Paste drain down test

A sieve and pan setup shown in Fig. 3 was used to perform the paste drain down test on the pervious concrete (PC) following the British Standards Institution (2000) guidelines [36]. This test visually assesses the paste's capacity to create a film around the aggregates. To conduct the test, 200 g of pervious concrete (PC) was extracted from the real mix and positioned in a 90-micron sieve. The sieve pan assembly was shaken for one minute using a sieve vibrator/shaker. If a considerable amount of paste accumulates in the pan, it suggests that the mix cannot form a strong membrane, and therefore, adjustments should be made to the mix design.

Workability

Although pervious concrete (PC) is considered zero-slump concrete, to assess the effect of nano-limestone (NL) on the workability of the pervious concrete (PC) slump test was conducted as per the standard procedure of ASTM C143 [37].The mould is to be filled in four layers, with each layer being compacted by applying twenty-five blows using a smooth-edged tamping rod. After filling, the mould should be removed slowly and cautiously in a vertical motion. Pervious concrete might settle, and the extent of this settling, known as slump, should be promptly gauged by measuring the variation between the initial height of the mould and the settled sample height.

Hardened density

The approach described in C1754/C1754M (ASTM International, 2012) [38] was employed to ascertain the hardened density of all pervious concrete (PC) mixes (with and without nano-limestone (NL). The procedure involved placing the sample in an oven at 105 °C for 24 h until a consistent weight was reached. The weight of the dried specimen (W_{dry}) and its volume (V) were then recorded to calculate the density of the pervious concrete (PC) using Eq. (1). The ultimate hardened density of the pervious concrete (PC) was determined by averaging the results from three pervious concrete (PC) specimens. Equation (1) demonstrates that the hardened density (D) is obtained by dividing the ovendry mass of the specimen (W_{dry}) in kilograms by the specimen's volume (V) in cubic meters.

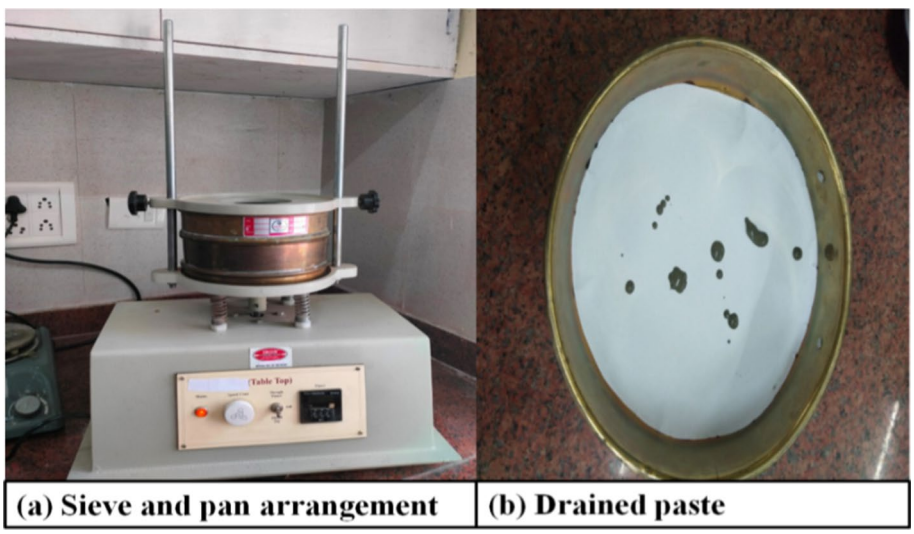

Fig. 3 Paste drain down test

$$D = \frac{W_{\text{dry}}}{V} \tag{1}$$

Porosity

The testing procedure laid out by ASTM International (2012) [38] is followed to determine the porosity of all pervious concrete (PC) mixes (with and without NL). The specific gravity bench determines cylindrical specimen's underwater weight (W2). The sample is positioned in a wire bucket and weighed after 10 min of submergence in water. After measuring the underwater weight, the same specimen is dried in an oven at 105C° for 24 h, and the weight of the dried sample in the air is noted as W1. The porosity is calculated using Eq. (2), which considers the weight of the sample in dry and submerged conditions, the volume of the sample, and the apparent density of water. Three samples from each batch of pervious concrete (PC) are employed to calculate the porosity, and the average of these values is reported as the final porosity of the pervious concrete (PC).

$$P = \left[1 - \frac{(\text{W1} - \text{W2})}{V\rho w}\right] \times 100 \tag{2}$$

Mechanical properties

The mechanical properties of the pervious concrete (PC), like compressive, splitting tensile, and shear strength, were estimated after 3, 7, 14, and 28 days of curing. The compressive strength test was done on cube specimens of 150 mm in size on CTM (3000 KN) as per the specifications laid down in BIS 516 (1959) [39]. A consistent loading rate of 5.2 KN/s was upheld throughout all the compression tests. The maximum load (P) causing the specimen's failure was recorded, and the compressive strength (f_c) was determined using Eq. (3). The ultimate compressive strength of the sample was reported as the average compressive strength from three specimens,

$$f_c = \frac{P}{A} \tag{3}$$

where P represents the maximum load, and A denotes the specimen's cross-sectional area.

A splitting tensile strength test was performed on UTM (1000 KN) having two point loading system after 3, 7, 14, and 28 days of curing; for this purpose, cylindrical specimens of size $h = 300$ mm and $d = 150$ mm were cast as per the guidelines of IS: 5816 [40]. Tensile strength was determined using Eq. (4):

$$T = \frac{2P}{\pi DL} \tag{4}$$

Here, T represents the tensile strength measured in MPa, P denotes the maximum applied load in KN, and D and L stand for the diameter and length of the sample in m, respectively.

The investigation followed previous studies [41] and conducted shear strength tests on pervious concrete at 3, 7, 14, and 28 days of curing. To achieve this, L-shaped specimens were cast. Figure 4a–d illustrates all the conducted tests. The test involved inserting a $150 \times 90 \times 60$ mm wooden block into a 150 mm cube specimen. Support was provided by 12 and 22 mm diameter mild steel rods and

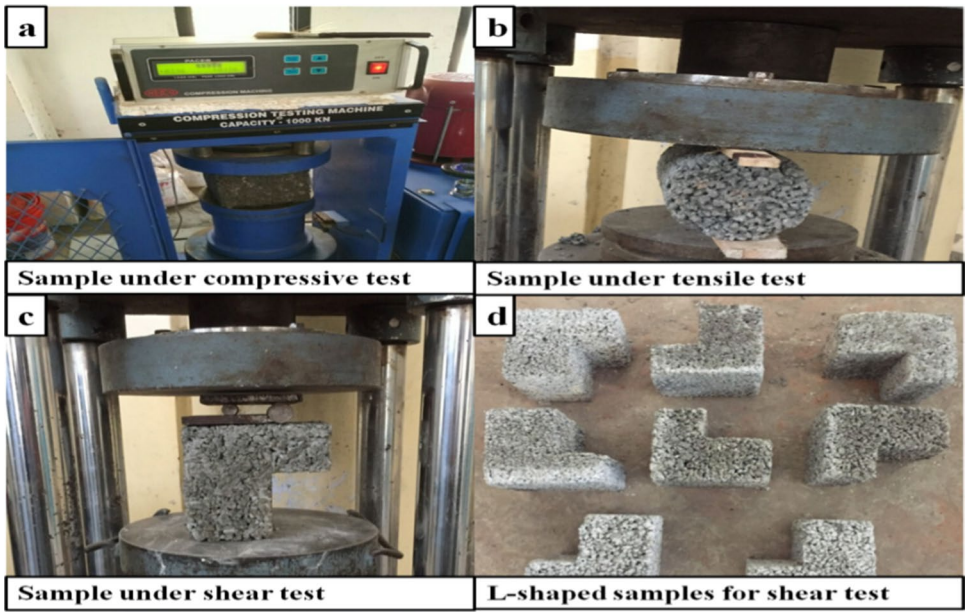

Fig. 4 **a** Compressive strength test, **b** split tensile strength test, **c** shear strength test, and **d** L-shaped specimens for shear strength testing

two plates (150 × 110 × 10 mm and 150 × 85 × 10 mm). The arrangement created a shear plane beneath the 22-mm rod. To achieve accurate shear strength results, the loading rate was kept below 140 kg/cm^2 per minute to ensure precise shear failure.

Infiltration properties

The infiltration rate of pervious concrete (PC) mixes, both with and without nano-limestone (NL), was determined following the guidelines provided by ASTM (C 1701/C 1701 M-09) was adopted in our previous studies [42]. To conduct the tests, cylindrical moulds, as illustrated in Fig. 5, were utilised, featuring a diameter of 300 mm and a height of 450 mm. These moulds are designed to facilitate the casting and testing processes without needing external ring or support. The moulds were marked with three lines to establish reference points for the infiltration testing. The first line, positioned 300 mm from the bottom of the specimen, denotes the maximum level of pervious concrete. The second line is marked 10 mm above the first line, indicating the minimum water level during the test. The third line, situated 15 mm above the second line, represents the maximum water level. These reference lines were crucial for maintaining the proper water level throughout the infiltration test. The head, or water level, should be maintained during the test between the second and third marked lines. To calculate the infiltration rate of water through the pervious concrete, Eq. (5) was employed:

$$I = \frac{(K \times M)}{(D^2 \times t)} \tag{5}$$

In the equation:

I denotes the infiltration rate in millimetres per second (mm s^{-1}), M represents the mass of water in kilograms (kg). D represents the diameter of the cylindrical mould in millimetres (mm). K is the permeability rate constant, and t indicates the time in seconds (s). This equation provides a quantifiable measure of the rate at which water infiltrates the pervious concrete sample.

Microstructural analysis

Mineralogical analysis of all designed mixes was performed on a very advanced X-ray diffractometer (XRD) Rigaku SmartLab. For morphological analysis, Zeiss Gemini-500 FE-SEM with very less system vacuum of 4.6e$^{-0.5}$ was used. To enhance the conduciveness, samples were initially gold coated on quorum Q150R S plus and then analysed. To analyse the modifications caused by the functionalities of pervious concrete (PC) with incorporation nano-limestone (NL), the composition and development of hydration phases within the pervious concrete (PC) incorporated with nano-limestone (NL) was investigated through Fourier transform infrared spectroscopy (FT-IR) using Shimadzu QATR-S 28 after 28 days of curing. This analytical technique allowed for the examination of the specific chemical bonds and structures formed during the hydration process in the concrete, providing insights into the interaction of nano-limestone (NL) during hydration.

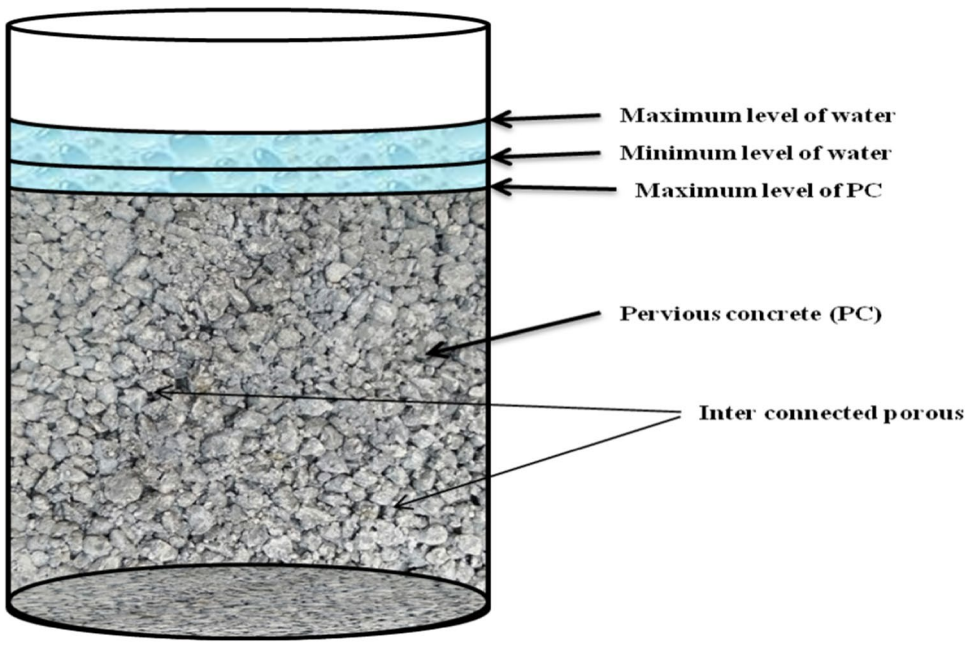

Fig. 5 Cylindrical mould for casting and testing

Results and discussion

This section will provide an overview of the findings and analyses of pervious concrete (PC) strength, infiltration, and microstructural characteristics with and without nano-limestone (NL). The fresh properties of pervious concrete (PC), which include workability and paste drain down assessments, were performed right after creating the pervious concrete (PC) mixes, while the other evaluations were carried out at distinct curing periods, as previously stated. In other words, the tests were conducted at different times after the pervious concrete (PC) mixes were prepared to observe the evolution of the pervious concrete (PC) properties over time. This approach was taken to understand how pervious concrete (PC) and modified pervious concrete (PC) behave and how their properties change over time.

Paste drain down test

The paste drain test, a visual examination performed in the study, was utilised to evaluate the bleeding of cement paste in pervious concrete. All pervious concrete mixes were subjected to this test, as depicted in Fig. 6. Previous research has indicated that the capacity of cement paste to form a membrane or flow smoothly can significantly impact the performance of pervious concrete. The ability of cement paste to form a membrane and its rheology can also affect the distribution of cement paste and pore structure in pervious concrete [43]. The test findings indicated that adding nano-limestone (NL) can help control paste bleeding to an acceptable level. In mix PC0NL, adding fine aggregates improved the workability of pervious concrete but weakened the bond at the interfacial zone due to a decrease in paste thickness. However, using nano-limestone (NL) in the other four pervious concrete (PC) mixes helped to control paste bleeding with a small reduction in workability. Incorporating 1% and 2% of nano-limestone (NL) in the mix provided acceptable results of paste bleeding, but the mix with 3% and 4% of nano-limestone (NL) incorporation experienced minimal drainage due to an increased proportion of nano-limestone (NL). The specific surface area of the admixture affects the paste thickness, and nano-limestone (NL) has a high specific surface area that helps form a smooth and uniform membrane around the aggregates and enhances paste thickness. However, an augmentation in the thickness of the cement paste can lead to an increase in compressive and splitting tensile strength. But If the thickness of the cementitious paste exceeds a certain limit, and it can lead to the formation of concrete without any voids. This, in turn, renders pervious concrete ineffective as it contradicts its intended purpose, and the same is reported for PC3NL and PC4NL during infiltration and porosity tests.

Workability

The slump value of pervious concrete (PC) is typically low, but adding a small amount of fine aggregates significantly

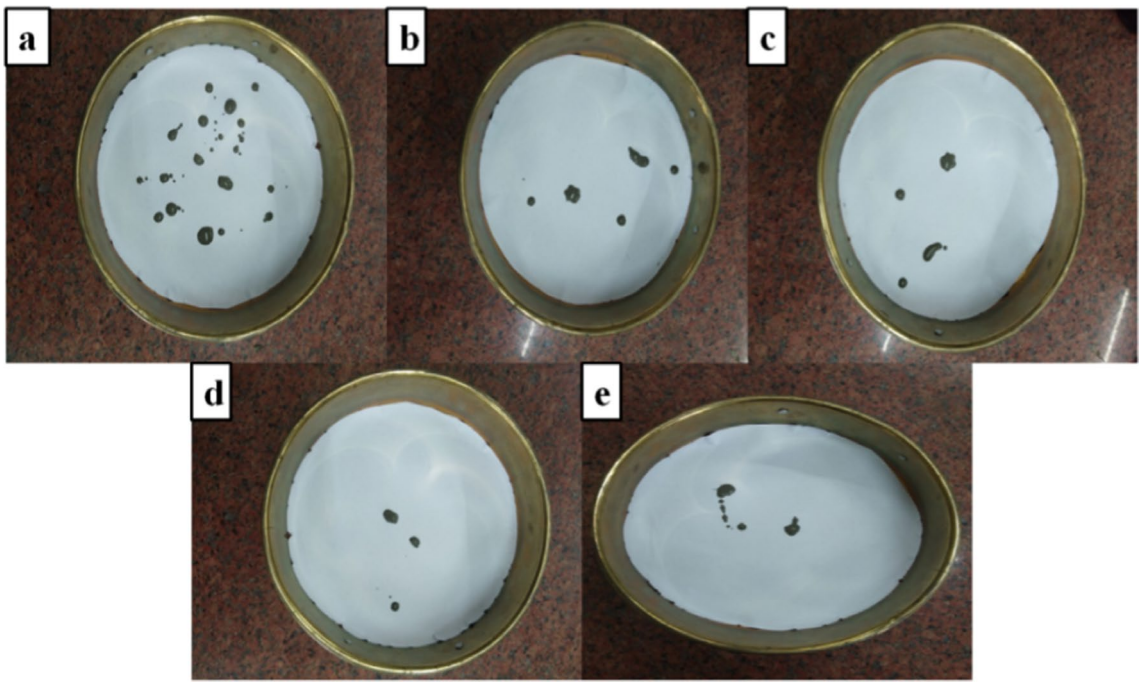

Fig. 6 Paste drains down test of all PC mixes. **a** PC0NL, **b** PC1NL, **c** PC2NL, **d** PC3NL, and **e** PC4NL

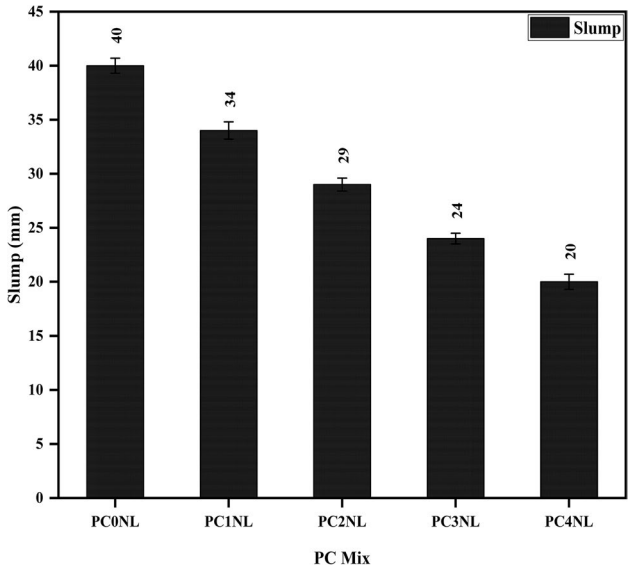

Fig. 7 Slump values of all mixes

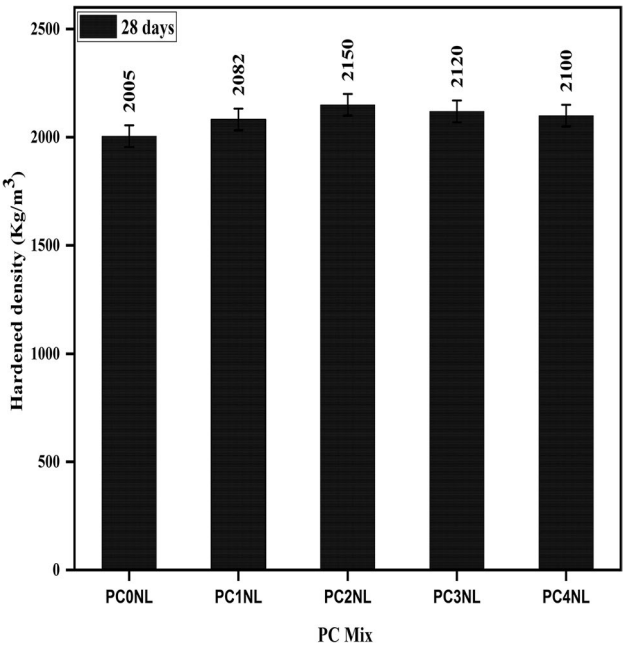

Fig. 8 Density of all mixes

improved it. The inclusion of FA densifies mix matrix offers more lubricative surface area and improves workability. Figure 7 shows the slump values of all pervious concrete mixes tested. In the first phase, the control mix PC0NL with 0% nano-limestone (NL) content had a slump value of 40 mm. In the second phase, 34 mm, 29 mm, 24 mm, and 20 mm slump values were observed in PC1NL, PC2NL, PC3NL, and PC4GO, respectively. It is clear from Fig. 7 that the slump values of pervious concrete (PC) decrease as the percentage of cement replaced by nano-limestone (NL) increases. The maximum 50% reduction in slump value was observed in mix PC4NL with 4% nano-limestone (NL) content compared to the normal mix. The decrease in workability in pervious concrete (PC) mixes can be credited to nano-limestone (NL) high surface area-to-volume ratio [22]. As the percentage of nano-limestone increases, the surface area available for water–cement interaction also increases. This leads to higher water demand for hydration, reducing the water-to-cement ratio. Reduced water content has a direct impact on the fluidity of pervious concrete, diminishing its workability. It means that when there is less water in the mixture, the concrete becomes less workable. This effect has been observed consistently in prior research studies [44, 45], which also reported comparable findings.

Hardened density

The findings of this investigation, illustrated in Fig. 8, demonstrate that the pervious concrete mixes have an absolute hardened density ranging from 2025 to 2165 kg/m^3, which is lower than the standard density of traditional concrete at 2400 kg/m^3. The disparity in density can be attributed to the higher porosity level observed in pervious concrete. Moreover, the figure accompanying the findings reveals that the density of hardened pervious concrete exhibits an upward trend as the proportion of nano-limestone (NL) in the mix increases. The pervious concrete with 0% nano-limestone (NL) (PC0NL) has the least absolute density. Furthermore, incorporating nano-limestone (NL) results in a significant increment in the absolute density of pervious concrete relative to the control mix (PC0NL), which comprises 100% OPC. For example, mix PC1NL with 1% nano-limestone (NL) exhibits a 3.8% increase in density compared to the control mix (PC0NL).

Similarly, mix PC2NL with 2% nano-limestone (NL) shows a 7.2% increase in absolute hardened density. The mixes PC3NL and PC4NL, which contain 3%, and 4%, nano-limestone (NL), respectively, also exhibit an increase in absolute hardened density of 5.7% and 4.7%, but less compared to mix with 2% of nano-limestone (NL). Adding nano-limestone (NL) modifies the particle packing in pervious concrete, resulting in a denser matrix packing and a consequent increase in hardened density. Furthermore, using nano-limestone (NL) enhances the hardened density by filling both micro and nano-pores, leading to the densification of the pervious concrete. The increase in hardened density up to a certain percentage of nano-limestone (NL) replacement (2%) suggests the positive impact of nano-limestone on the packing and interlocking of cementitious particles, leading to improved compaction. However, beyond this optimum replacement level, the hardened density slightly decreased. This could be attributed to an excessive addition

of nano-limestone (NL), resulting in overcrowding of particles and reduced interparticle interactions. Factors such as agglomeration of NL particles or insufficient mixing may also contribute to the observed variation in hardened density.

Porosity

Porosity using conventional methodology

The results of porosity for the six mixes examined in this study are presented in Fig. 9. The measured values of porosity ranged from 11.2% to 17.9%, which is within the acceptable range except for the mix PC3NL and PC4NL according to the guidelines provided by ACI. Therefore, based on the recommended porosity range of 15%-35% in ACI 522R-10, 2010 [15], all the designed mixes investigated in this study were categorised as pervious concrete except mix PC3NL and PC4NL as they possess porosity of less than 15%. Hence, these two mixes can be categorised as low-permeable concrete. The highest porosity value was observed in mix PC0NL, while the lowest was in mix PC4NL. Porosity is influenced by various factors, such as the size of the aggregate, the proportion of fine aggregates, and the amount of binder content, which is a volumetric characteristic. A higher cement by aggregate (C/A) ratio in pervious concrete (PC) led to decreased porosity, which can be attributed to increased cement content. The increase in the cement content increased the packing density of the matrix, which resulted in a decrease in porosity. In the same manner, an increase in the amount of fine content led to a decrease in porosity due to an increase in packing density.

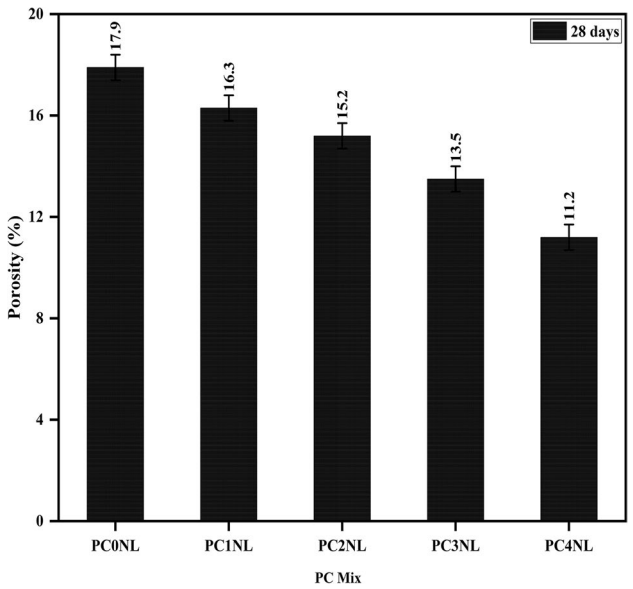

Fig. 9 Slump values of all mixes

However, in all the mixes of pervious concrete (PC), the C/A ratio, amount of fine aggregates, and aggregate gradation were the same. Therefore, the porosity of the pervious concrete (PC) mixes was determined solely by the percentage of nano-limestone (NL) incorporation. The mix with 0% nano-limestone (NL) content, PC0NL, had the highest porosity value of 17.9%, while the mix with 4% nano-limestone (NL) content, PC4NL, had the lowest porosity value of 11.2%. This is because nano-limestone (NL) acts as nano-reinforcement, which densifies the pervious concrete (PC) at the nano level, reducing porosity.

Porosity through CT scanning technique

The CT scan conducted on optimal pervious concrete mix PC2NL revealed a total porosity of 15.7% and a connected porosity of 14.9%. This indicated that the pervious concrete sample possesses a significant volume of void spaces, enabling the easy passage of water. The CT scan images in Fig. 10 illustrate a well-interconnected network of voids throughout the pervious concrete (PC) matrix, highlighting its high permeability and drainage capabilities. The total porosity of 15.7% demonstrated the substantial void volume present within the sample, while the connected porosity of 14.9% indicated the proportion of voids that are effectively interconnected, allowing for efficient water to infiltrate. The CT scan and porosity tests provide different insights into the material's porosity. While the CT scan test offers detailed imaging of internal structures, the porosity test quantifies the porosity percentage. In this case, there is a difference of 3.3% in porosity between the results obtained from these two tests, findings from the CT scan closely aligned with the results obtained from the porosity test.

Description of compressive strength and splitting tensile strength

The compressive strength of all the mixes was evaluated after 3, 7, 14, and 28 days, respectively. The cured moulds were directly placed under CTM till the cubes failed. Concrete strength is directly related to how dense the structure has become after proper curing, which depends upon the formation of hydration products like C-S, C-S-H gel, and pore refinement [46]. The pervious concrete (PC) has shown a desirable effect on compressive strength while replacing the cement with a proper replacement amount of nano-limestone (NL).

The study shows that at 1% and 2% replacement of cement by nano-limestone (NL), there is a rapid increase in early 3-day strength of pervious concrete (PC) up to 40.11% and 48.20%, respectively, similarly for other curing days 7, 14, and 28 days the improvement in strength was recorded as 26.7%, 19%, 14.2%, and 33.2%, 25.2%,

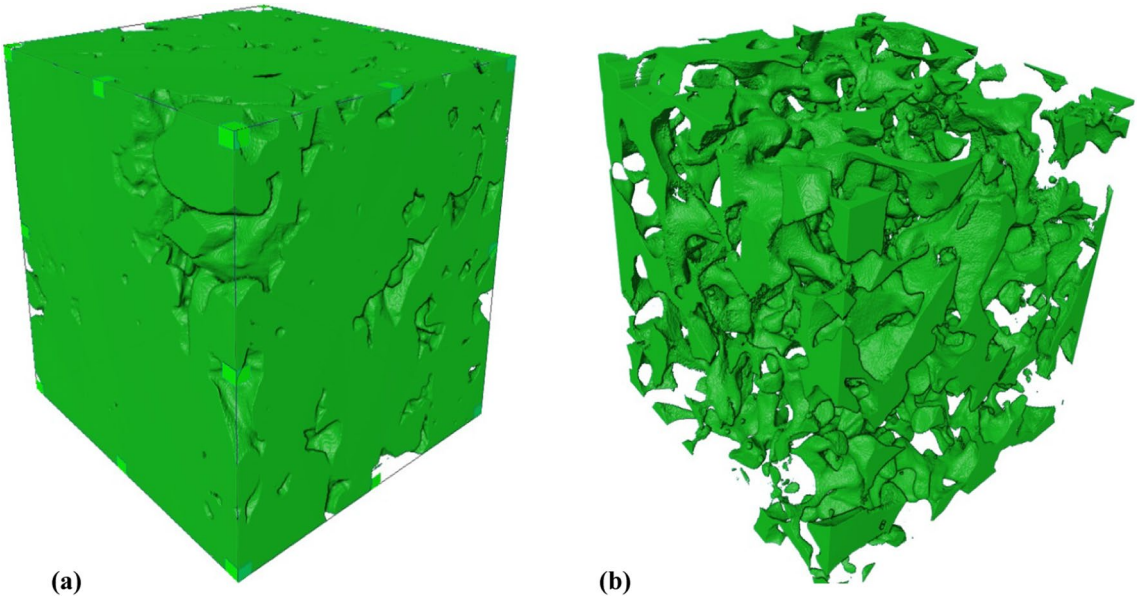

Fig. 10 **a** PC sample before CT scan, **b** PC sample after CT scan

19.2%, respectively, than normal pervious concrete PC0NL (0% nano-limestone (NL)). Similarly, for other replacement rates of 3% and 4%, very less improvement was recorded as 19%, 18.8%, 10.6%, 12.6%, and 14.4%, 13.7%, 9.5%, 5.9% at 3, 7, 14, and 28 days of curing period. A more pronounced nucleation effect of nano-limestone (NL) at early ages may account for the substantial variation in strength increase of pervious concrete (PC) with and without nano-limestone (NL) between early and later ages, notably for PC1NL and PC2NL. The study also reveals that 2% of nano-limestone (NL) is the optimum replacement for cement in pervious concrete. At 3% and 4% replacement, the strength shows a declining trend in the compressive strength of the pervious concrete (PC). Although adding more nano-limestone (NL) than 2% led to a decrease in strength is unidentified; it could be because of the increased filler and dilution effect. Figure 11 shows the compressive strength of different mixes for 3, 7, 14 and 28-days cured specimens, respectively, the findings drawn align entirely with prior research conducted in the field, particularly in studies referenced as [47–49]. These earlier studies have also highlighted and supported the significance of proper nano-limestone replacement and dispersion for enhancing concrete properties. The current findings substantiate and reinforce the consensus established by these previous studies, emphasising the critical role of effective dispersion techniques, such as those mentioned, in optimising concrete performance through nano-material incorporation.

Figure 12 illustrates that the split tensile strength results exhibit a consistent pattern that aligns with the trend observed in the compressive strength results concerning the control pervious concrete (PC) mix; the two types of strength testing yield similar findings regarding their relationship with the control pervious concrete (PC) mix. Likewise, in compressive strength, the inclusion of nano-limestone (NL) in pervious concrete (PC) has significantly enhanced its splitting tensile strength. This improvement was observed during all standard curing periods (3, 7, 14, and 28 days) compared to pervious concrete (PC) without nano-limestone (NL) under the normal curing condition at 0.35 water/cement ratio. It can be observed from Fig. 12 at 2.0% nano-limestone (NL) replacement; the pervious concrete (PC) exhibited a remarkable increase in split tensile strength by approximately48.6%, 23.8%, 18.8%, and 16.4% at 3, 7, 14, and 28 days compared to the control pervious concrete (PC) mix. Similarly, at 1% of nano-limestone (NL) replacement, the splitting tensile strength improved by around 38.5%, 15.1%, 14.2%, and 12.3% at 3, 7, 14, and 28 days compared to the control pervious concrete (PC) mix. However, as the nano-limestone (NL) content reached 3% and 4.0%, the degree of enhancement gradually decreased compared to the mix with 1% and 2% of nano-limestone (NL). The minimal increase in strength of mix with 3% nano-limestone (NL) was recorded as 17.4%, 8.7%, 7.5%, and 9.3%, respectively, at 3, 7, 14, and 28 days, similarly for mix with 4% nano-limestone (NL) the minimal increase in strength was observed as 5.5%, 1.7%, 1.2%, and 2.6% at 3, 7, 14, and 28 days, respectively. Thus, there is an optimal amount of nano-limestone (NL) nano-limestone (NL), around 2%, which significantly enhances the pervious concrete (PC) compressive and split tensile strengths. The enhancement of strengths by incorporating nano-limestone

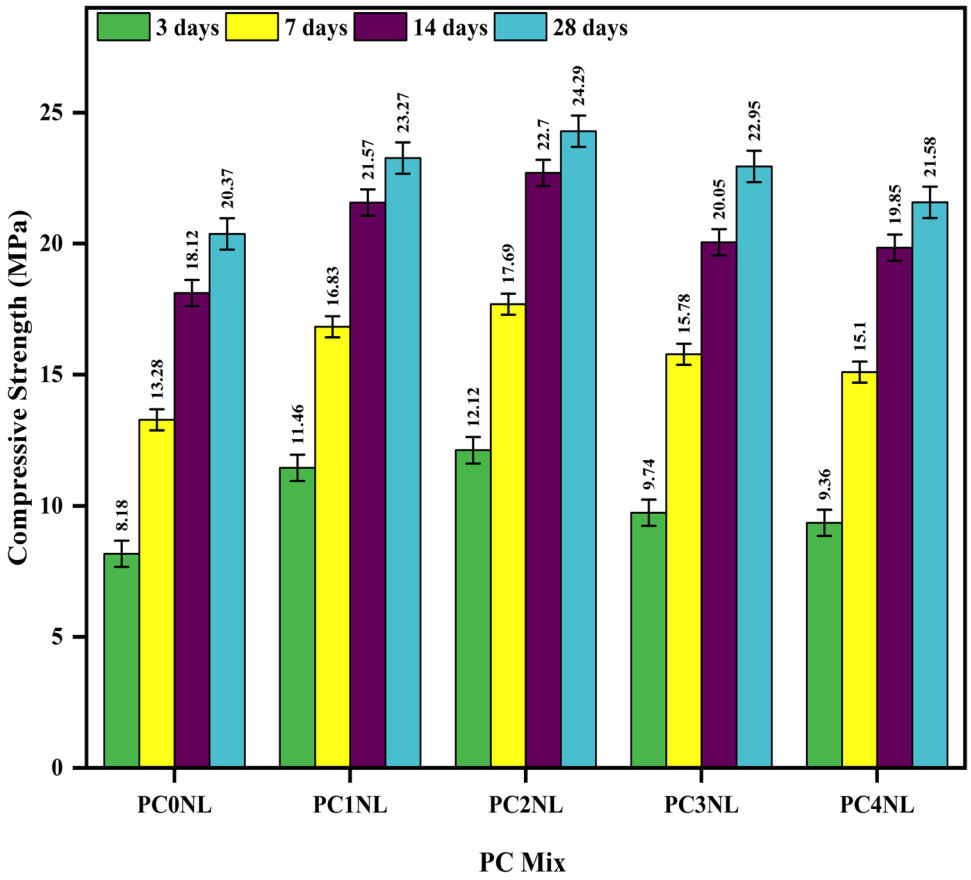

Fig. 11 Compressive strength test results for all mixes

(NL) can be credited to the nucleation effect induced by the nano-limestone (NL) particles.

Furthermore, nano-limestone acts as an inert filler, creating a dense microstructure in pervious concrete (PC) through improved packing and aiding in early cement hydration, and there is a threshold (2%) beyond which the strength may be negatively affected. This threshold can be understood as a result of two compensating effects triggered by the nano-limestone (NL) particles: Acceleration and dilution, and the lack of uniform dispersion of nano-limestone (NL) particles, leading to the entrapment or reduction in workability during slump tests. This observation also suggests that the inclusion of nano-limestone (NL) aids in the compounds like calcium carbo-aluminates and calcium carbo-silicates, which contribute to the enhanced strength properties of the pervious concrete (PC). The findings were evident from the visual evidence provided by the FE-SEM micrographs in Fig. 18 and the hydration products formed during the hydration process analysed through XRD and FT-IR analysis in Fig. 19.

Figure 13 compares compressive and splitting tensile strengths for different pervious concrete mixes, both with and without nano-limestone (NL). Based on the coefficient of determination (R^2) value of 0.97, it is evident that there exists a strong linear relationship between these two variables. The test results for splitting tensile strength and compressive strength of various pervious concrete specimens, with and without nano-limestone (NL), follow the same trend. The correlation between compressive and splitting tensile strength has also been supported by earlier research [44]. It is also possible to predict the splitting tensile strength in future based on our developed prediction model.

Relation between compressive strength and infiltration with NL percentage

The ideal relationship between nano-limestone (NL) % with compressive strength and infiltration rate is shown in Fig. 14. The pervious concrete (PC) without nano-limestone (NL) and with varied nano-limestone (NL) % is represented by the PC mix in the abscissa. Compressive strength and nano-limestone (NL) percentage have a strong quadratic relationship with an R^2 value of 0.95, but the infiltration rate has a negative linear relationship ($R^2 = 0.99$).

Shear strength

The results in Fig. 15 illustrate the average shear strength values of different mixes of pervious concrete, produced with or without nano-limestone (NL), at various curing

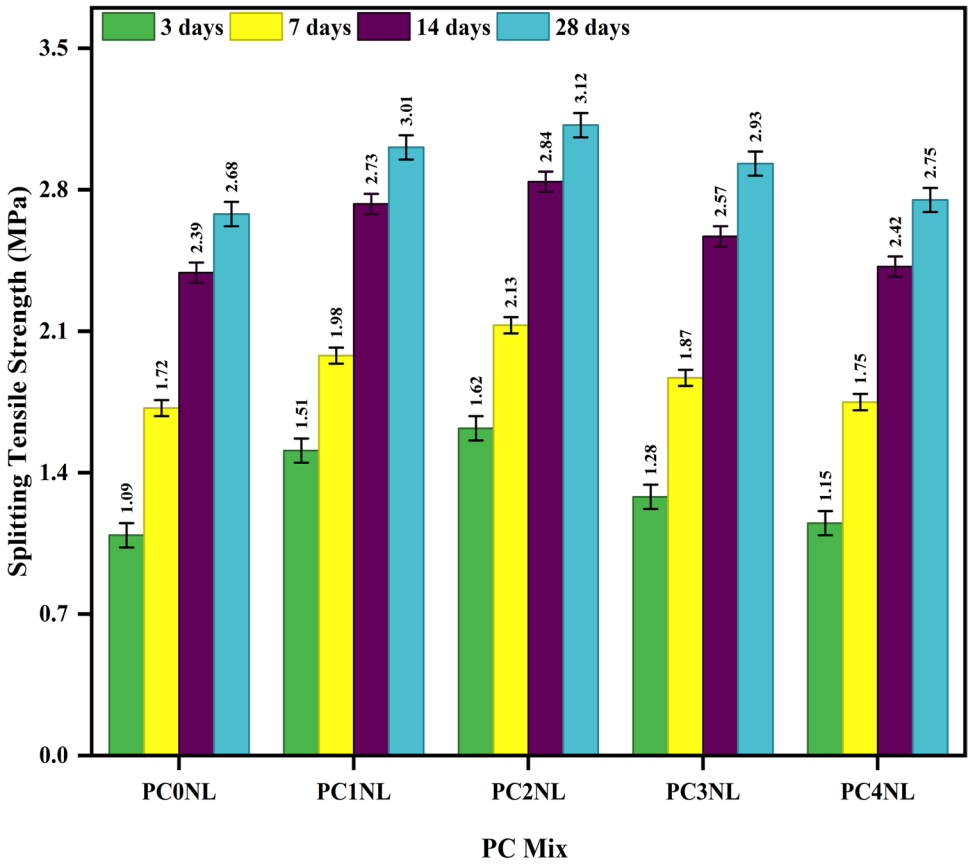

Fig. 12 Splitting tensile strength results for all mixes

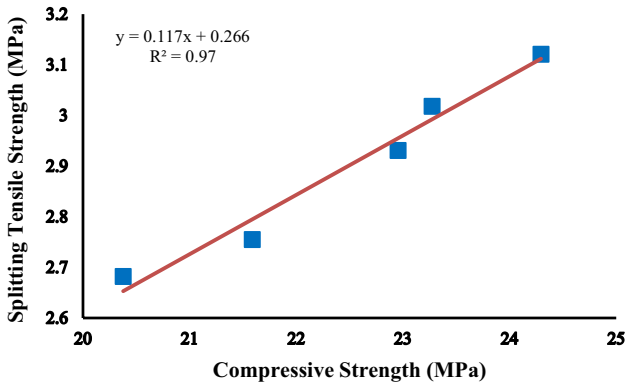

Fig. 13 Relationship between compressive strength and splitting tensile strength

ages (3, 7, 14, and 28 days), using L-shaped specimens. The primary aim of this investigation was to determine the ductility and brittleness of the material. The results indicated a significant increase in the shear strength of all pervious concrete mixes with an increase in the concentration of nano-limestone (NL) compared to the control mix, which is composed entirely of OPC. For example, the mix PC1NL, which contains 1% of nano-limestone (NL), showed a substantial increase in shear strength of 46.2%, 17.6%, 9%, and 17.6% at 3, 7, 14, and 28 days of the curing period, respectively, when compared to the control mix. As the percentage of nano-limestone (NL) increased, the shear strength of the pervious concrete mix exhibited a continuous rise. The mixture PC2NL, containing 2% nano-limestone (NL) demonstrated a notable increase in shear strength of 58.6%, 28.8%, 14.6%, and 26.4%at 3, 7, 14, and 28 days of the curing period, respectively, in comparison to the control mix. The results indicated that the increase in shear strength can be attributed to the higher degree of packing density resulting from the presence of nano-limestone (NL) in the mix. This improved the bridging contact between the paste and aggregates and aided in the fast hydration of cement particles, as evidenced by the FE-SEM micrographs in Fig. 18. Additionally, mixes with higher percentages of nano-limestone (NL) (PC3NL and PC4NL) showed a minimal percentage increase in shear strength of 20.6%, 13.9%, 4%, 8.4%, and 3.3%, 4.1%, 1.7%, 2%, at 3, 7, 14, and 28 days of curing, respectively. After 3 days of curing, a significant increase in shear strength was observed compared to the control mix; the same was observed during compressive and split tensile strength testing. The mix containing 2% of nano-limestone (NL) exhibited the highest peak level of shear strength among all the pervious concrete mixes tested.

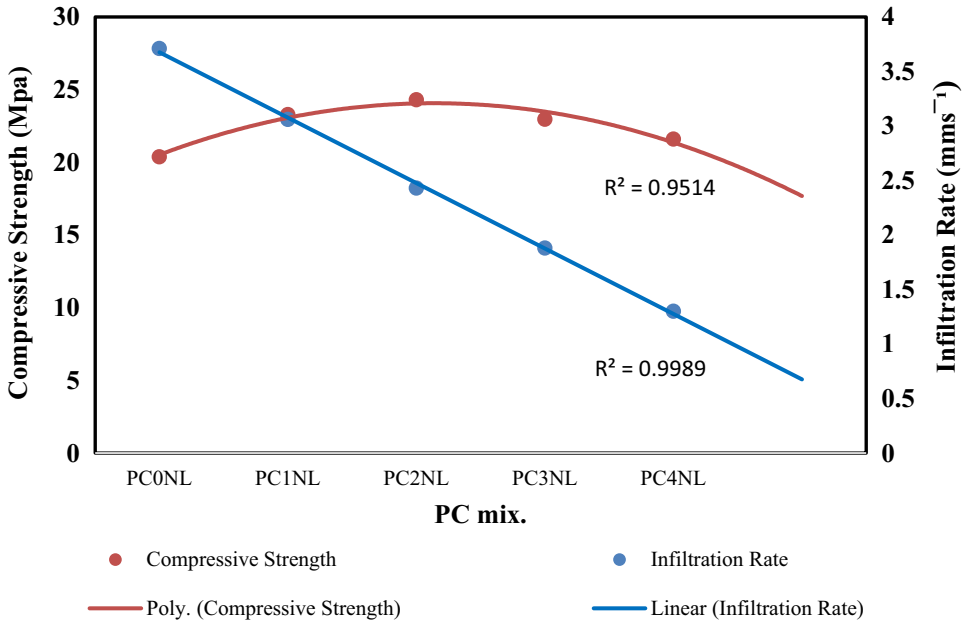

Fig. 14 Correlation of compressive strength and infiltration rate with NL percentage

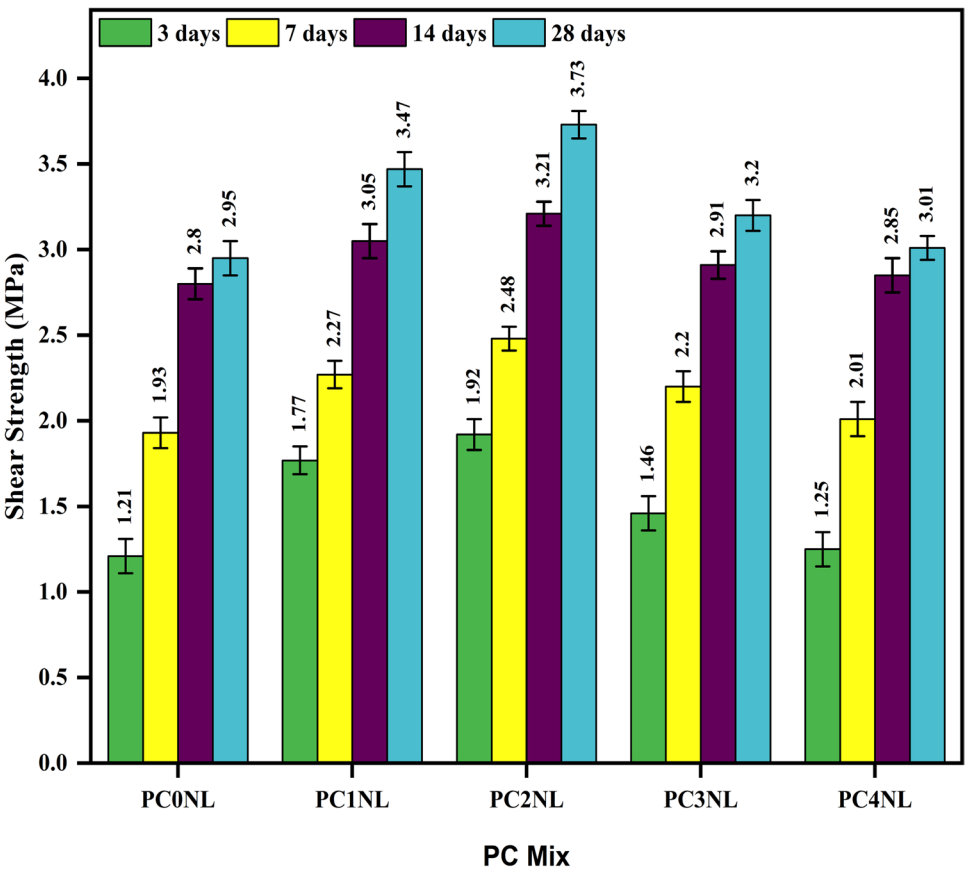

Fig. 15 Shear strength results for all mixes

Description of infiltration

All the mixes infiltration properties were checked per the procedure following ASTM (C 1701/C 1701 M-09) [42] after 28 days using laboratory apparatus. For this purpose, cylinders with the Mix design presented in Table 3 were casted, and curing of the composite was done for 28 days. The casted moulds were directly placed below the outlet

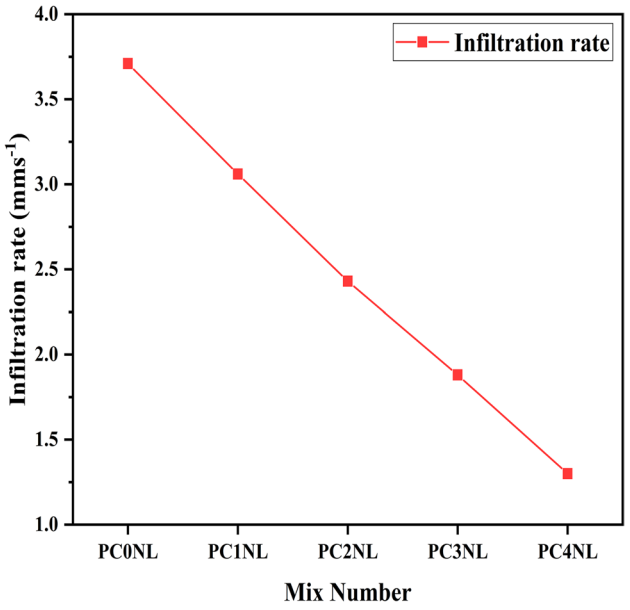

Fig. 16 Infiltration rate for all mixes

gate of the device, and a fixed (40 lb) of water was allowed to pass through the concrete matrix; simultaneously, the time was recorded for the complete infiltration of 40 lbs of water. The infiltration rate for every mix was observed and recorded; the results are presented in Fig. 16. It was observed as the amount of nano $CaCO_3$ increased, the pervious concrete (PC) became less permeable for PC0NLinfiltration rate was 3.71 mm s^{-1} and for PC4NL, it was only 1.30 mm s^{-1}. A prominent decrement of 65% infiltration rate (IR) was recorded for mix PC4NL (4% nano-limestone (NL)).

Similarly, for mix PC1NL (1% NL), PC2NL (2% NL), and PC3NL (3% NL), the percentage reduction in infiltration was observed as 17.5%, 34.5%, and 49.3% compared to control mix PC0NL (0% nano-limestone (NL)), respectively. Though at 1% and 2% replacement, the infiltration rate of the composite decreased, it was within the standard permeable range than PC3NL and PC4NL as per (ACI 522R-10, 2010) [15]. The reduction in infiltration rate can be explained by the decrease in porosity resulting from an increase in the proportion of nano-limestone (NL), as demonstrated by the porosity test and by CT scan presented in Figs. 9 and 10. Additionally, nano-limestone (NL) functions as a potent catalyst that hastens the hydration process and alters the nano-level pore structure. Moreover, in this study, the experimental observation of a uniform membrane created by nano-limestone (NL) surrounding the aggregates with better rheological properties during the paste drain down test presented in Fig. 6 suggests that this mechanism could contribute to densifying the pore structure at the nano-level by enhancing bonding. A correlation was established between the infiltration rate (IR) and porosity of all the pervious concrete (PC) mixes, indicating that the initial infiltration rate of pervious concrete (PC) can be estimated based on the measured porosity, as depicted in Fig. 17, with an R^2 value of 0.97.

Microstructural analysis

To analyse the modifications in the microstructure of PC (with and without nano-limestone (NL)) responsible for improving the properties of pervious concrete by observing the interaction interface, generally called interfacial transition zone (ITZ), after 28 days of curing, which can be understood from the physicochemical characterisation of nano limestone interaction with the matrix of the pervious concrete using FE-SEM, FT-IR, and XRD analysis. The study revealed that when cement is replaced with an adequate percentage of nano $CaCO_3$ the physicochemical properties are improved. Since the findings of the compressive, shear, and splitting tensile strength and infiltration testing strongly suggested that a replacement rate of 2% was ideal, the other replacement rates (1%, 3% and 4%) of nano $CaCO_3$ were excluded from this analysis, several other studies [50, 51] supported this decision.

FE-SEM analysis

It can be observed from Fig. 18a the specimen (PC0NL) without nano-limestone (NL) exhibits a significant presence

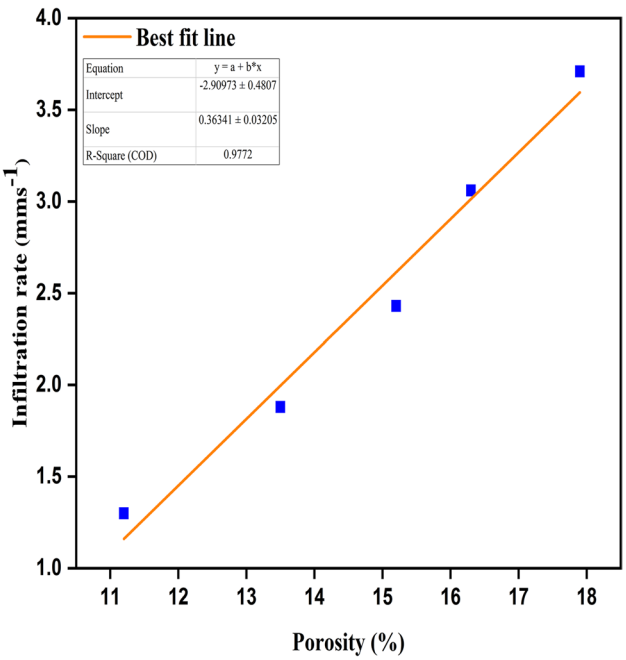

Fig. 17 Correlation between IR and porosity

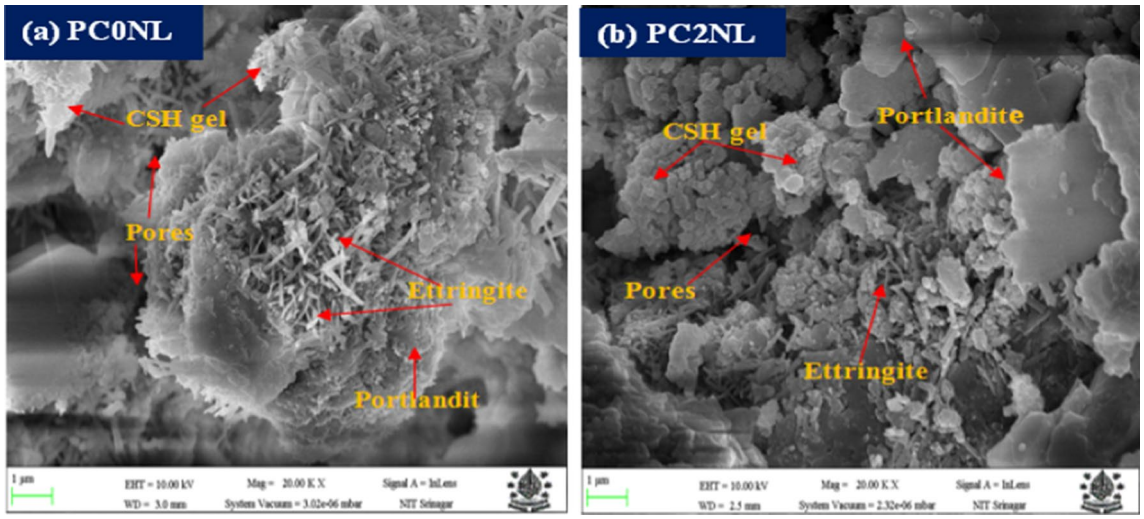

Fig. 18 FE-SEM micrographs of **a** PC0NL, **b** PC2NL at 28-days curing

of well-built porous areas along with calcium hydroxide plates. However, the inclusion of nano-limestone (NL) acts as a filler and effectively occupies the pores, resulting in a denser microstructure in the pervious concrete (PC) matrix, as depicted in Fig. 18b mix PC2NL (2% nano-limestone (NL)). This denser microstructure is attributed to the particle packing effect of nano-limestone (NL). The replacement of cement by nano-limestone (NL) has a boundary nucleation growth effect, which accelerates the hydration reaction by offering more surfaces for nucleation and growth of hydration products C-S–H (grey impression), enhances cement hydration which directly accounts for the improved strength of nano $CaCO_3$ pervious concrete (PC) (PC2NL). Figure 18b indicates that nano-limestone (NL) appears to expedite the cement hydration and diminish ettringite formation within the pervious concrete (PC) matrix. This suggests that nano-limestone (NL) enhances the chemical reactions in cement curing, leading to a more efficient and controlled hydration process. Additionally, reducing ettringite formation is beneficial, as excessive ettringite can cause potential durability issues in concrete.

Figure 18 highlights that the ettringite crystals for pervious concrete with nano-limestone (PC2NL) are reduced but are much larger compared with PC0NL pervious concrete without nano-limestone (NL), which supports the increase in the early hydration process. Their presence leads to an increase in the early compressive strength of the pervious concrete (PC). Nano-limestone (NL) provides nucleation sites for CSH precipitation, facilitates cement hydration, and improves packing by filling nano-pores, which accounts for the improved strength of nano-limestone (NL) pervious concrete (PC2NL), the findings are in line with [49, 52]. Hence, the decrease in permeability for the pervious concrete (PC2NL) compared to (PC0NL) might be due to the dense structure revealed in PC2NL compared to PC0NL during the analysis.

XRD analysis

To study the hydration products formed during the hydration process, the X-ray diffraction (XRD) analysis was carried out on PC-powered specimens with and without nano-limestone (NL) after 28 days of curing age, as shown in Fig. 19a the presence of calcium silicates (CS1), calcium alumino-silicates hydrates (CA1), ettringite (E), and portlandite (P) were observed in the main phases. As nano-limestone (NL) could not generate other crystals, no major change for normal and modified mixes was observed in phase composition. This suggests that the nano-limestone particles did not undergo substantial chemical reactions or generate new compounds during hydration. Nevertheless, the observed improvements in the mechanical properties and microstructure can be attributed to the physical effects of nano-limestone, such as enhanced packing and improved interparticle bonding. In addition, the diffraction peaks of quartz (Q) were also observed as relics of fine and coarse aggregates. The disclosures are in line with the previous reported results [47, 53]. The conversion of calcium hydroxide into secondary CSH gel in modified mix PC2NL can be observed from a decrease in intensity count, resulting in increased strength of modified pervious concrete (PC). Peaks of portlandite were found at 18.122, 35.310, 47.011, and 50.920, and that for ettringite were found at 15.655 and 34.211as presented in Fig. 19a.

FT-IR analysis

FT-IR was used to analyse the infrared absorption spectrum for pervious concrete (PC) with and without nano-limestone

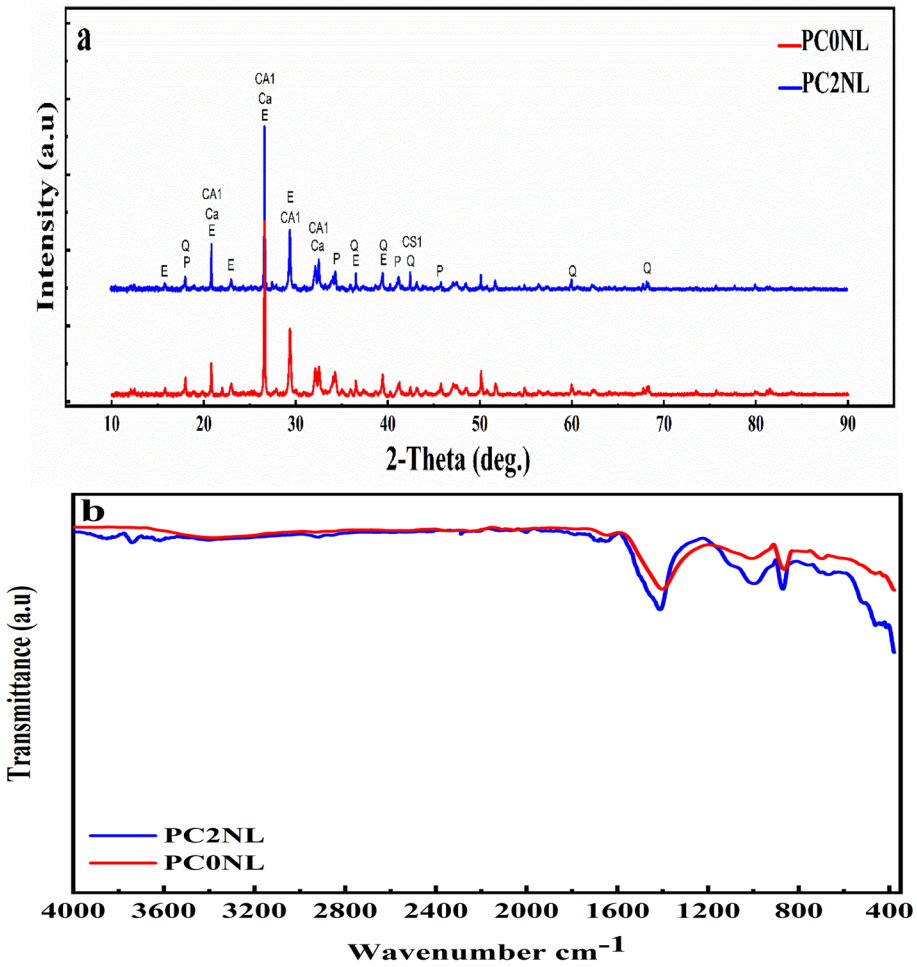

Fig. 19 The spectrum of PC0NL and PC2NL through **a** XRD, **b** FT-IR at 28-days

(NL). The results are presented for PC0NL and PC2NL after 28-day curing. The test was conducted with sixteen scans with a resolution of 1 cm^{-1} and the range of optical frequency ranged (400–4000 cm^{-1}). Figure 19b shows the spectrum of 28-day hardened pervious concrete (PC) with no and 2% (w/w) nano limestone. The FT-IR spectrum can be categorised into two main zones (for both PC0NL and PC2NL), symmetric stretching vibrations between 4000 and 1600 cm^{-1} and asymmetric bending and stretching vibrations between 1600 and 400 cm^{-1}. The peaks around 3640 cm^{-1} are attributed to the presence of the −OH (hydroxyl) functional group of portlandite. The wide bands observed between 3450 and 1635 cm^{-1}, and 1667 cm^{-1} are due to hydrated silicates. The asymmetric bedding in PC0NL near 970 cm^{-1} due to Si–O is credited to the developing of CSH crystals. The absorbance bands show increased peaks for PC2NL compared to the normal pervious concrete (PC) samples, particularly around 978 and 1500 cm^{-1}. The absorbance bands observed in PC2NL around 950 cm^{-1} are attributed to the asymmetric stretching of Si–O bonds by the new material added. However, the bending and stretching of the band around 1500 cm^{-1} are attributed to the vibrations of atomic water present in the concrete. However, a comparative analysis of the FT-IR spectra did not indicate any significant changes or additional peaks associated with chemical interactions between the nano-limestone and the cementitious matrix of pervious concrete (PC). This suggests that the modifications observed in pervious concrete's mechanical, infiltration properties, and microstructure are primarily attributed to physical effects rather than chemical reactions. The absence of major chemical interactions between nano-limestone (NL) and the cementitious matrix of pervious concrete (PC) is not surprising, considering the inert nature of nano-limestone (NL) and the relatively short duration of the hydration process. Nevertheless, the physical effects of nano-limestone, such as improved packing, enhanced inter-particle bonding, and densification, contribute to the overall enhancement of pervious concrete performance. The FT-IR results, in agreement with recent studies on nano-materials [54, 55], support the observation of minimal chemical interactions between nano-limestone (NL) and the cementitious matrix of pervious concrete (PC). It aligns with the inert nature of nano-limestone and the relatively short hydration duration, indicating that nano-limestone generally does not

induce significant chemical changes within the cementitious matrix.

Cost analysis

The compressive strength to total cost ratio, also known as the economic index (EI), is a crucial measure in the construction industry that evaluates the efficiency of a building material. This index is determined by dividing the material's compressive strength by the total cost. The higher the compressive strength to total cost ratio, the more economically efficient the material is. Therefore, the economic index is an essential metric for ensuring the long-term sustainability of building projects while keeping costs under control. In this study, the raw materials were purchased from the market, and nano-limestone (NL) was obtained from locally available limestone via pulverisation using a specially designed ball mill in the laboratory. This study found that a mix with 2% of nano-limestone (PC2NL) has a higher EI value, followed by a 1% nano-limestone (PC1NL) mix. However, the mixes with 3% and 4% nano-limestone (NL) have better EI values than those with 0% nano-limestone (NL). The minimum EI value of 0.00363 was observed in Mix PC0NL, similarly The EI values of 0.00417, 0.00438, 0.00417, and 0.00394 was observed in Mix PC1NL, PC2NL, PC3NL, and PC4NL. Mix PC2NL has a maximum of 0.00438 EI value, as presented in Table 5. Hence, According to the cost analysis, a mix with 2% nano-limestone (NL) was the optimum choice.

Conclusions

The study comprehensively explores properties of pervious concrete (PC) with the replacement of cement by nano-limestone (NL) to the extent of 4% by weight. The major conclusions drawn from the study are summarised as:

1. Replacement $\leq 2\%$ cement with nano-limestone (NL) improved strength in pervious concrete (PC) without impacting its permeability. Notably, at a 2% replacement level of nano-limestone (NL):
   - Maximum compressive strength of 12.12 MPa after 3 days and 24.29 MPa after 28 days was seen for mix PC2NL.
   - Maximum splitting tensile strength of 1.62 MPa and 3.12 MPa after 3 and 28 days was seen for mix PC2NL.
   - Maximum shear strength of 1.92 MPa and 3.75 MPa after 3 and 28 days was seen for the same mix, respectively,

   The percentage increase in compressive strength was observed as 48.20% at 3 days and 19.23% at 28 days. Similarly, splitting tensile and shear strength rose by 48.6%, 16.4%, and 58.6%, 26.4% at 3 and 28 days, in PC2NL, respectively, compared to the control mix PC0NL.
2. Beyond 2% replacement, increased nano-limestone (NL) content led to an increase in viscosity, hence infiltration rate decreased by 64.73% from mix PC0NL to mix PC4NL.
3. Comprehensive characterisation through FE-SEM, XRD, and FT-IR analyses revels denser micrographs, increased growth of hydration products and reduction of portlandite in modified mix PC2NL, affirming the nano-limestone (NL) role in enhancing pervious concrete's strength properties.
4. A direct positive correlation was established between infiltration and porosity, emphasising the importance of considering these factors in pervious concrete mix design. The highest values were achieved in PC0NL (3.71 mms^{-1}, 17.9%), while the lowest values were recorded in PC4NL (1.30 mms^{-1} and 11.2%), respectively.
5. Mix PC2NL demonstrated higher Economic index values, indicating its economic feasibility and potential practical applicability.

In summary, integrating nano-limestone (NL) into pervious concrete (PC) applications shows significant promise in advancing mechanical properties while considering infiltration rates and economic viability. These findings hold substantial implications for the practical utilisation of pervious concrete in diverse construction projects.

Table 5 Cost analysis for kg/m^3 of all mixes in Indian rupees

Mix. No	OPC (INR)	CA (INR)	FA (INR)	NL (INR)	Water (INR)	Total cost (INR)	CS (MPa)	EI (CS/cost)
PC0NL	3884.88	1457	259	0	7	5607.88	20.37	0.00363
PC1NL	3846.03	1457	259	3	7	5572.03	23.27	0.00417
PC2NL	3807.18	1457	259	6	7	5536.18	24.29	0.00438
PC3NL	3768.33	1457	259	9	7	5500.33	22.95	0.00417
PC4NL	3729.48	1457	259	12	7	5464.48	21.58	0.00394

Acknowledgements The authors are grateful to the National Institute of Technology, Srinagar, for providing the laboratory facility during the course of this research.

Author contributions GA performed methodology, original—draft writing, investigation and experiments, and editing. TR provided conceptualisation, visualisation, supervision, and review editing.

Declarations

Conflict of interest The authors confirm that they have no known financial or interpersonal conflicts that could have influenced the research presented in this study.

Ethical approval This article does not contain any studies with human participants or animals performed by any of the authors.

Informed consent For this type of study, formal consent is not required.

References

1. D'Armada P, Hirst E (2012) Nano-lime for consolidation of plaster and stone. J Archit Conserv 18:63–80
2. Boot-Handford ME, Abanades JC, Anthony EJ et al (2014) Carbon capture and storage update. Energy Environ Sci 7:130–218
3. Hanus MJ, Harris AT (2013) Nanotechnology innovations for the construction industry. Prog Mater Sci 58:1056–1102
4. Huang B, Wu H, Shu X, Burdette EG (2010) Laboratory evaluation of permeability and strength of polymer-modified pervious concrete. Constr Build Mater 24:818–823
5. Ibrahim A, Mahmoud E, Yamin M, Patibandla VC (2014) Experimental study on Portland cement pervious concrete mechanical and hydrological properties. Constr Build Mater 50:524–529
6. Deo O, Neithalath N (2011) Compressive response of pervious concretes proportioned for desired porosities. Constr Build Mater 25:4181–4189
7. Kevern JT, Wang K, Schaefer VR (2010) Effect of coarse aggregate on the freeze-thaw durability of pervious concrete. J Mater Civ Eng 22:469–475
8. Neithalath N, Sumanasooriya MS, Deo O (2010) Characterizing pore volume, sizes, and connectivity in pervious concretes for permeability prediction. Mater Charact 61:802–813
9. Yahia A, Kabagire KD (2014) New approach to proportion pervious concrete. Constr Build Mater 62:38–46
10. Sonebi M, Bassuoni M, Yahia A (2016) Pervious concrete: mix design, properties and applications. RILEM Tech Lett 1:109–115
11. Chandrappa AK, Biligiri KP (2016) Comprehensive investigation of permeability characteristics of pervious concrete: a hydrodynamic approach. Constr Build Mater 123:627–637
12. Chen Y, Wang K, Wang X et al (2013) Strength, fracture and fatigue of pervious concrete. Constr Build Mater 42:97–104
13. Tennis PD, Leming ML, Akers DJ (2004) Pervious concrete pavements. Portland Cement Association, Skokie, IL
14. Kia A, Delens JM, Wong HS, Cheeseman CR (2021) Structural and hydrological design of permeable concrete pavements. Case Stud Constr Mater 15:e00564
15. ACI Committee 522 (2010) Pervious Concrete: Report No. 522R-10, American Concrete Institute. Farmington Hills, Michigan, p 40
16. Juradin S, Netinger-Grubeša I, Mrakovčić S, Jozić D (2021) Impact of fibre incorporation and compaction method on properties of pervious concrete. Mater Constr 71:e245–e245
17. Lee J-W, Jang Y-I, Park W-S, Kim S-W (2016) A study on mechanical properties of porous concrete using cementless binder. Int J Concr Struct Mater 10:527–537
18. Norhasri MM, Hamidah MS, Fadzil AM (2017) Applications of using nano material in concrete: a review. Constr Build Mater 133:91–97
19. Ramadhansyah PJ, Mohd Ibrahim MY, Hainin MR, Wan Ibrahim MH (2014) A review of porous concrete pavement: applications and engineering properties. Appl Mech Mater 554:37–41
20. Singh LP, Karade SR, Bhattacharyya SK et al (2013) Beneficial role of nanosilica in cement based materials: a review. Constr Build Mater 47:1069–1077
21. Hosseini P, Hosseinpourpia R, Pajum A et al (2014) Effect of nano-particles and aminosilane interaction on the performances of cement-based composites: an experimental study. Constr Build Mater 66:113–124
22. Poudyal L, Adhikari K, Won M (2021) Mechanical and durability properties of portland limestone cement (PLC) incorporated with nano calcium carbonate ($CaCO_3$). Materials 14:905
23. Xavier CSB, Rahim A (2022) Nano aluminium oxide geopolymer concrete: an experimental study. Mater Today Proc 56:1643–1647
24. Sobolev K (2016) Modern developments related to nanotechnology and nanoengineering of concrete. Front Struct Civ Eng 10:131–141
25. Li W, Huang Z, Cao F, Sun Z, Shah SP (2015) Effects of nano-silica and nano-limestone on flowability and mechanical properties of ultra-high-performance concrete matrix. Constr Build Mater 95:366–374
26. Balaguru PN (2005) Nanotechnology and concrete: background, opportunities and challenges. In: Applications of nanotechnology in concrete design: proceedings of the international conference held at the University of Dundee, Scotland, UK on 7 July 2005. Thomas Telford Publishing, pp 113–122
27. Sato T, Beaudoin JJ (2007) The effect of nano-sized $CaCO_3$ addition on the hydration of cement paste containing high volumes of fly ash. In: Proceedings of the 12th international congress on the chemistry of cement, Montreal, Canada, pp 8–13
28. Ramezanianpour AA, Ghiasvand E, Nickseresht I et al (2009) Influence of various amounts of limestone powder on performance of Portland limestone cement concretes. Cement Concr Compos 31:715–720
29. Standard-IS, Indian (1987) IS 12269-1987: specifications for 53 grade ordinary Portland cement. IS, New Delhi
30. I. Standard, IS: 383 (2016) Coarse and fine aggregate for concrete-specification. Bureau of Indian Standards, New Delhi.
31. IS 456 (2000) Indian standard: plain and reinforced concrete—code of practice. Bureau of Indian Standards, New Delhi
32. Bureau of Indian Standards (BIS) (2002) IS: 2386 (Part V)-1963: methods of test for aggregates for concrete, Part V. Soundness, Indian Stand, pp 1–14.
33. IS: 2386 (Part IV) (2016) Methods of test for aggregates for concrete, Part 4: mechanical properties. Bureau of Indian Standards, New Delhi, pp 1–37
34. ASTM C131M-20 (2014) C131/C131M-14 standard test method for resistance to degradation of small-size coarse aggregate by abrasion and impact in the Los Angeles Machine, C. 04 5-8. https://doi.org/10.1520/C0131
35. ASTM C 128-01 (2001) Standard test method for density, relative density (specific gravity), and absorption. ASTM Int 88:1–6. www.astm.org.
36. British Standards Institution, BS EN 12350-1:2000 (2000) Testing fresh concrete
37. ASTM C 143/C 143M (2002) Standard test method for slump of hydraulic-cement concrete. In: Annual book of ASTM standards, vol 04.02. American Society for Testing and Materials, Philadelphia

38. ASTM International (2012) C1754/C1754-12: standard test method for density and void content of hardened pervious concrete. Annual Book of ASTM Standard, p 3
39. BIS (1959) 516 Method of tests for strength of concrete. Bureau of Indian Standards, New Delhi, India
40. IS 5816-1999 Method of test for splitting tensile strength of concrete. Bureau of Indian Standards, New Delhi, India.
41. Simalti A, Singh AP (2020) Comparative study on direct shear behavior of manufactured and recycled shredded tyre steel fiber reinforced self-consolidating concrete. J Build Eng 29:101169
42. Standard A (2009) C1701/C1701M-09 standard test method for infiltration rate of in place pervious concrete. ASTM International, West Conshohocken, PA
43. Muhammad NZ, Keyvanfar A, Zaimi M et al (2015) Waterproof performance of concrete: a critical review on implemented approaches. Constr Build Mater 101:80–90
44. Singh D, Singh SP (2020) Influence of recycled concrete aggregates and blended cements on the mechanical properties of pervious concrete. Innov Infrastruct Solut 5:1–12
45. Kevern JT, Schaefer VR, Wang K (2011) Mixture proportion development and performance evaluation of pervious concrete for overlay applications. ACI Mater J 108:439–448
46. Mohamed A, Khaled AH (2015) Effect of using different types of nano materials on mechanical properties of high strength concrete. Constr Build Mater 80:116–124
47. Bhat AH, Naqash JA (2022) Experimental studies of sustainable concrete modified with colloidal nanosilica and metakaolin. J Build Pathol Rehabil 7:18
48. Vinoth P, Nallasamy P, Tomar AK et al (2021) An experimental investigation on pervious concrete replacement with silica. Int J Res Eng Sci 9:20–25
49. Camiletti J, Soliman AM, Nehdi ML (2013) Effects of nano-and micro-limestone addition on early-age properties of ultra-high-performance concrete. Mater Struct 46:881–898
50. Mishra S, Tiwari A (2016) Effect on compressive strength of concrete by partial replacement of cement with nano titanium dioxide and nano calcium carbonate. J Civil Eng Environ Technol 5:426–429
51. Shaikh FU, Supit SW, Barbhuiya S (2017) Microstructure and nanoscaled characterization of HVFA cement paste containing nano-SiO_2 and nano-$CaCO_3$. J Mater Civ Eng 29:04017063
52. Bonavetti VL, Rahhal VF, Irassar EF (2001) Studies on the carboaluminate formation in limestone filler-blended cements. Cem Concr Res 31:853–859
53. Ramezanianpour AA, Jovein HB (2012) Influence of metakaolin as supplementary cementing material on strength and durability of concretes. Constr Build Mater 30:470–479
54. Heikal M, Abd El Aleem S, Morsi WM (2013) Characteristics of blended cements containing nano-silica. HBRC J 9:243–255
55. Delgado AH, Paroli RM, Beaudoin JJ (1996) Comparison of IR techniques for the characterization of c`onstruction cement minerals and hydrated products. Appl Spectrosc 50:970–976